Mathematical Biosciences and Engineering

MBE, 19 (12): 12936–12949.
DOI: 10.3934/mbe.2022604
Received: 16 June 2022
Revised: 10 July 2022
Accepted: 24 July 2022
Published: 05 September 2022

http://www.aimspress.com/journal/MBE

Research article

A model for analyzing evolutions of neurons by using EEG waves

Massimo Fioranelli[1], O. Eze Aru[2], Maria Grazia Roccia[1], Aroonkumar Beesham[3,4] and Dana Flavin[5]

[1] Department of Human Sciences, Guglielmo Marconi University, Via Plinio 44, 00193 Rome, Italy
[2] Department of Computer Engineering, College of Engineering and Engineering Technology, Michael Okpara University of Agriculture, Umudike Umuahia, Abia State, Nigeria
[3] Faculty of Natural Sciences, Mangosuthu University of Technology, PO Box 12363, Jacobs 4026, South Africa
[4] Department of Mathematical Sciences, University of Zululand, Private Bag X1001, Kwa-Dlangezwa 3886, South Africa
[5] President, Foundation for Collaborative Medicine and Research, Greenwich CT, USA

* **Correspondence:** Email: profeze.aru14@gmail.com.

Abstract: It is known that differences between potentials of soma, dendrites and different parts of neural structures may be the origin of electroencephalogram (EEG) waves. These potentials may be produced by some excitatory synapses and currents of charges between neurons and then thereafter may themselves cause the emergence of new synapses and electrical currents. These currents within and between neurons emit some electromagnetic waves which could be absorbed by electrodes on the scalp, and form topographic images**.** In this research, a model is proposed which formulates EEG topographic parameters in terms of the charge and mass of exchanged particles within neurons, those which move between neurons, the number of neurons and the length of neurons and synapses. In this model, by knowing the densities of the frequencies in different regions of the brain, one can predict the type, charge and velocity of particles which are moving along neurons or are exchanged between neurons.

Keywords: EEG; brain; topography; frequency; wave; charges

1. Introduction

As of now, it is known that neurons build some electronic circuits which emit or absorb waves.

These waves could play the main role in imaging [1–3]. To detect and measure these waves, several techniques have been proposed. For example, electroencephalography (EEG) is one of the important tools for studying the electrical and temporal dynamics of the human brain's large-scale neural circuits in some diseases like Alzheimer's [4,5]. Modern EEG source imaging simultaneously details the electrical, temporal and spatial dimensions of brain activity, making it an important and affordable tool to consider the properties of cerebral, neural networks in cognitive and clinical neurosciences [6]. In fact, EEG microstates could characterize the resting-state activity of the human brain. Also, they represent the basic building blocks of the chain of spontaneous conscious mental processes, and their occurrence and temporal dynamics determine the quality of mentation [7]. In addition, these EEG microstates could be age-dependent, and may predict cognitive capacities in healthy individuals across their lifespan [8]. These states could have different applications, e.g., by using EEG microstates and considering the evolution of the brain, one can ascertain why some persons remember dreams and recall them and others cannot [9]. Also, by using EEG signals, autism spectrum disorder could be diagnosed very well [10,11]. In addition, (EEG) signal analysis can be well suited for the automated diagnosis of Alzheimer's disease [12].

Besides these applications, EEG topography may provide a rich metric by means of which one can understand the functioning of the brain [13]. For example, the topography of EEG power and the activation of brain structures during slow wave-sleep under normal conditions and after sleep deprivation could be considered. A research group indicated that sleep deprivation resulted in an increase in wave strength only for mid-delta activity, mainly in parietal and frontal regions [14]. Another group found the persistent enhancement in non-rapid eye movement (NREM) delta power especially in the frontal the parietal regions, and progressive increases in individual slow wave slope and frontal fast oscillation power [15]. Also, in parallel, many other works have been done on EEG topography. For example, one work proposed a method that transforms EEG (electroencephalography) signals to topographic images that contain the frequency and spatial information and utilizes a convolutional neural network (CNN) to classify the emotion, as CNN has improved feature extraction capability [16]. Another work has defined a unified time-frequency energy algorithm that makes topographical representation (ETR) robust in classifying multiple objects. Compared with existing EEG topology generations, the proposed method could be accurate and functional for spatial location, temporal onset, and stability simultaneously [17]. Other investigators have considered the role of EEG oscillations in predicting the presence or absence of dream recall (DR) by "state-" or "trait-like" factors [18].

All of these considerations have shown very useful applications of EEG waves in imaging. However, some questions remain. For example, what is the relation between EEG frequencies and the number of cells, molecules and charges? Or what is the relation between waves and thickness of scalp in different ages and parts of the brain? Also, how we could ignore or remove the effects of noises? In this research, we try to respond to all of these questions. Motivated by these researchers, we propose a model to formulate the EEG topographic results. We will consider the physical basis of features and neural evolution within the brain. Firstly, we will propose a simple model and then we generalize it to include all parameters.

The outline of paper is as follows: In section II, we consider the origin of brain waves and propose a model to formulate them. In section III, we test the model using experimental data. In section IV, we generalize the model and consider the effects of noises on the real data. The last section is devoted to a conclusion.

2. Method

In this section, we propose a model which considers the origin of radiated waves of the brain. We also calculate the frequencies and related probabilities.

In this model, a brain is built up from many neural circuits. Some synapses or charges induce electrical potentials within different parts of the neurons. Consequently, some differences between potentials of soma, dendrite and other parts appear. Each neuron has several gates which send or receive charges. The motion of charges within the neuronal structures and also between neurons produce some electrical currents. These currents emit some electromagnetic waves (see Figure 1). To calculate the frequency of these waves, firstly, we should calculate the magnetic fields which are produced by the motion of charges near the gate j of neuron i:

$$B_{ij} = \mu_0 \frac{I_{ij}}{2\pi r_{ij}} \tag{1}$$

where i is the index (related to position) of the neuron and j is the index (related to position) of the related gate (receptor, terminal or transmitter) of neuron i. In fact, each neuron (for example, neuron i) has several gates, including receptors, terminals or transmitters which are specified by j. Also, B_{ij} is the magnetic field at point ij of the brain which could be divided into two magnetic fields:

$$B_{ij} = B_{ij}^{'} + B_{ij}^{''} \tag{2}$$

where $B_{ij}^{'}$ is the magnetic field around a neuronal structure at point ij of the brain, $B_{ij}^{''}$ is the magnetic field around the synapse, r_{ij} is the distance from the point ij and I_{ij} is the current which could be obtained from the equation below:

$$I_{ij} = Q_{ij} V_{ij} \tag{3}$$

where Q_{ij} is the charge of the particles at point ij and V_{ij} is the velocity of the charges which are obtained from the equation below:

$$V_{ij} = \frac{l_{ij}}{T_{ij}} \tag{4}$$

Here, l_{ij} is the length of a neuron + the distance between two neurons at point ij and T_{ij} is the time needed so that the charges pass this distance. This magnetic field produces the energy density below at point ij:

$$U_{ij} = \frac{B_{ij}^2}{2\mu_0} \tag{5}$$

To obtain the total energy at point ij, we should multiply the density above and the volume at this point:

$$E_{ij} = \lambda_{ij} U_{ij} \pi r_{ij}^2 l_{ij} \tag{6}$$

where λ_{ij} is a volume dependent parameter. However, each neuron may oscillate and consequently, we will have the energy below:

$$r_{ij} \to r_{ij} + x$$

$$E_{ij} = \lambda_{ij} U_{ij} \pi (r_{ij} + x)^2 l_{ij} \tag{7}$$

To obtain the force at point ij of the brain, we should take the derivative with respect to x:

$$F_{ij} = \frac{dE_{ij}}{dx} = 2\lambda_{ij} U_{ij} \pi (r_{ij} + x)\ l_{ij} = k_{ij} x + cons\tan t \tag{8}$$

This force causes the oscillation of charges and produces the following frequency of the waves:

$$\nu_{ij} = \frac{1}{2\pi}\sqrt{\frac{k_{ij}}{m_{ij}}} = \frac{1}{2\pi}\sqrt{\frac{2\lambda_{ij} U_{ij} \pi l_{ij}}{m_{ij}}} = \frac{1}{2\pi}\sqrt{\frac{2\frac{\lambda_{ij} B_{ij}^2}{2\mu_0}\pi l_{ij}}{m_{ij}}} = \frac{1}{(2\pi)^2}\sqrt{\frac{\lambda_{ij}\mu_0 \pi l_{ij}}{m_{ij}}}\frac{Q_{ij}}{r_{ij}}\frac{l_{ij}}{T_{ij}} \tag{9}$$

To obtain the mean frequency in one region of the brain, we should sum over all frequencies and divide them into the number of frequencies:

$$\bar{\nu} = \frac{\sum n_i x_j \nu_{ij}}{\sum_{i,j=1}^{N,X} n_i x_j} \tag{10}$$

where X is the number of gates and N is the number of neurons. The probability for emission of each frequency can be obtained from the equation below:

$$P_{\nu_{ij}} = \frac{n_i x_j}{\sum_{i,j=1}^{N,X} n_i x_j} \tag{11}$$

Comparing these probabilities and frequencies with real experimental data, one can calculate the number of gates and neurons, the charges and masses of the particles and the distances between the neurons.

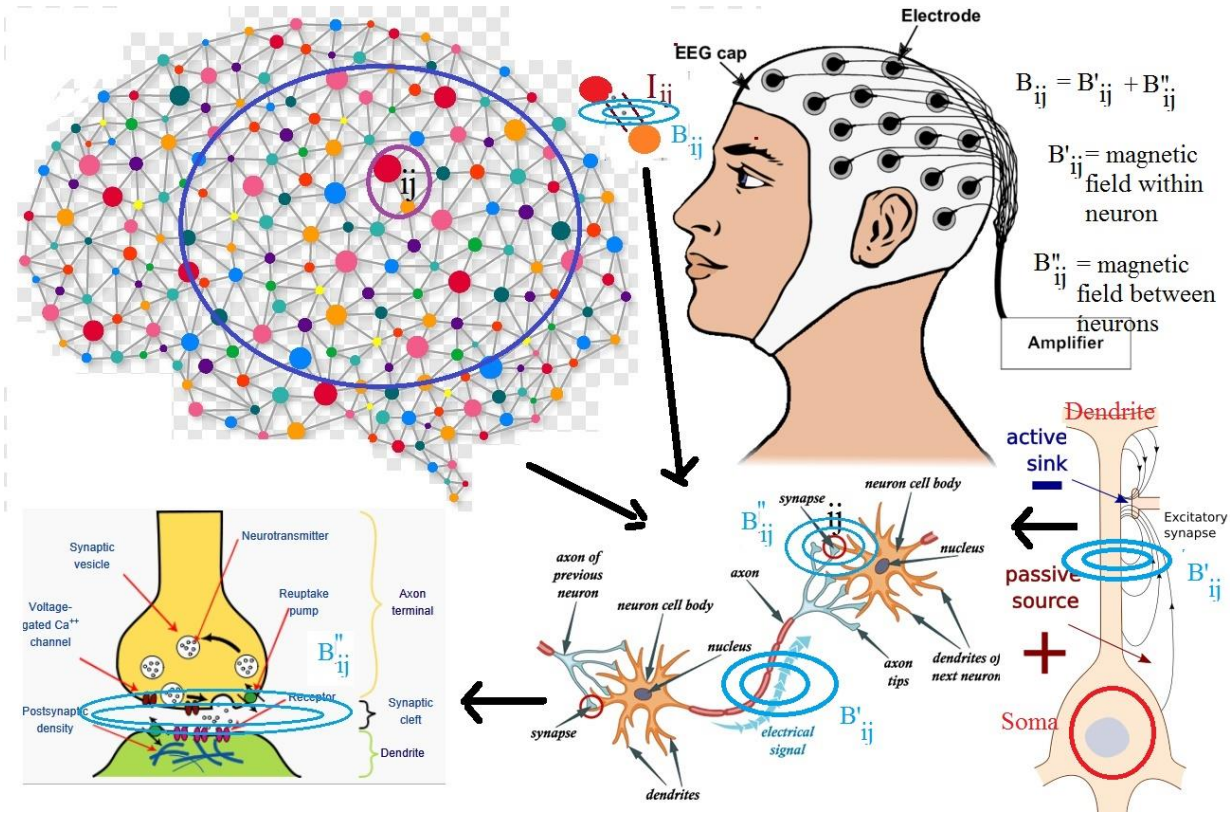

Figure 1. Emission of electromagnetic waves from electrical currents within neurons and exchanged charges between neurons.

3. Results

In this section, we will compare the model with experimental data and obtain some of the main parameters like the lengths of the neurons and synapses, and the number of neurons which interact with each other. For example, in Figure 2, we present the results of topographic EEG images for different brain waves during a dream. Using these results, we provide two tables and Figure 3.

Table 1 shows that if exchanged particles within neuronal structures or between neurons along the synapse length of calcium with charge +2 and mass 40.078 u, the distance between the dendrite and axon terminals (synapse lengths + neuron size) could be between 24-40 nanometers. Also, the radius of the circle which interactions occur around the axon-dendrites should change from 15.2 to 22.5 micrometers. For these results, at least 0.033 and at most 0.084 of the total number of neurons should enter into the interactions. The time of each interaction may be between 0.03 and 0.5 milliseconds.

Table 2 shows that by reducing the charges of the particles within the neuronal structures or exchanged particles between neurons to half for potassium channels, the number of interacting neurons, lengths of synapses and time of interactions should increase whilst the radii of the circles in which interactions occur, should decrease.

Figure 3 shows that for re-obtaining the same results in figure 2, by increasing the masses of particles with respect to a standard mass like the sodium mass, the number of interacting neurons should increase. This is because massive charges could not move fast and emit a smaller number of waves, and for this reason, to compensate for this reduction, we need more neurons to interact, exchange particles and charges and produce waves.

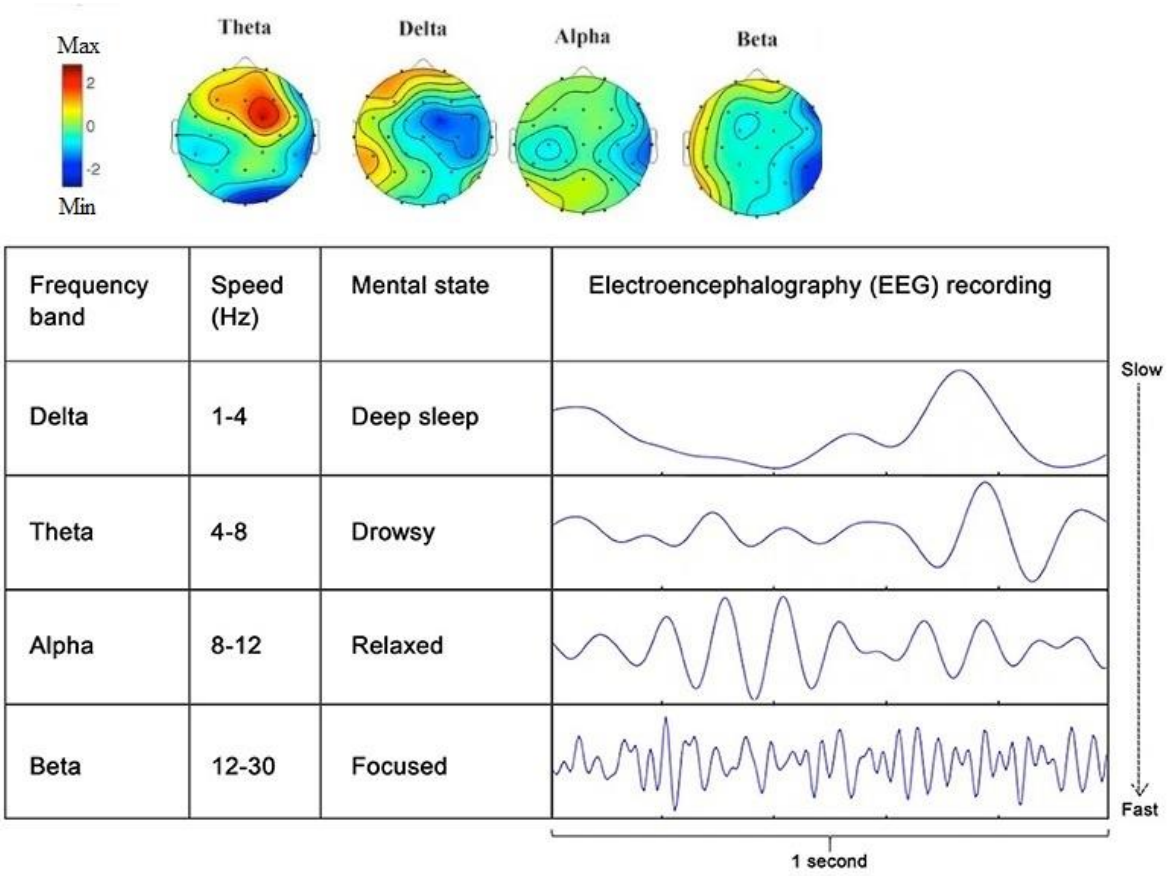

Figure 2. Topographic EEG images for different brain waves during a dream [1–18].

Table 1. Predicted estimates for charge, mass, length of synapses+ size of neurons, radius of interaction, number of neurons and calcium channels obtained from topographic EEG images in Figure 1.

	Q	m	l	r	N/N_{cri}	X/X_{cri}	T
Delta	**+2**	40.078 u	**32nano-meter**	**18.4 micro-meter**	**0.065**	**0.48**	**0.5 milli-second**
Theta	**+2**	40.078 u	**40nano-meter**	**15.2 micro-meter**	**0.084**	**0.66**	**0.12 milli-second**
Alpha	**+2**	40.078 u	**24nano-meter**	**22.5 micro-meter**	**0.033**	**0.24**	**0.08 milli-second**
Beta	**+2**	40.078 u	**28nano-meter**	**20.1 micro-meter**	**0.046**	**0.35**	**0.03 milli-second**

Table 2. Predicted estimates for charge, mass, length of synapses +size of neurons, radius of interaction, number of neurons and Potassium channels obtained from topographic EEG images in Figure 1.

	Q	m	l	r	N/N_{cri}	X/X_{cri}	T
Delta	**+1**	39.0983 u	**38nano-meter**	**16.2 micro-meter**	**0.072**	**0.68**	**0.33 milli-second**
Theta	**+1**	39.0983 u	**44nano-meter**	**13.2 micro-meter**	**0.123**	**0.83**	**0.09 milli-second**
Alpha	**+1**	39.0983 u	**27nano-meter**	**20.4 micro-meter**	**0.055**	**0.36**	**0.06 milli-second**
Beta	**+1**	39.0983 u	**30nano-meter**	**18.4 micro-meter**	**0.065**	**0.44**	**0.02 milli-second**

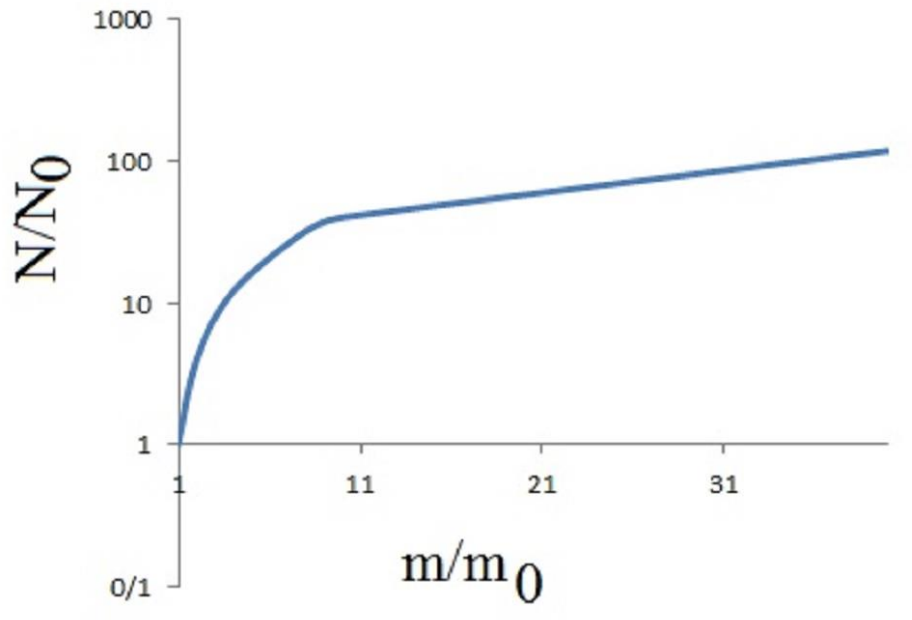

Figure 3. Increasing needed number of neurons by increasing mass of charges which move along neurons or are exchanged between neurons. Here, m is the mass of charges and m_0 is the standard mass.

4. A generalized version of the model

Until now, we have proposed a model which could determine frequencies and some parameters of EEG waves. However, we ignored the effects of noises which emerge from radiated electromagnetic waves from other neurons. We also should consider the effects of the distance between electrodes and neuronal sources, and the excitation of molecules which are located between them.

Firstly, suppose that a neuronal gate at point i and j of the brain produces an electrical current and this current emits a wave with the frequency and energy below:

$$E_{i_0 j_0} = h\,\nu_{i_0 j_0} \tag{12}$$

When this wave propagates on a circle, its energy should be divided on the circle with the center of the source and a radius which stretches from the center to each point. In these conditions, we have the energy below at each new point:

$$E'_{i_1 j_1} = \frac{E_{i_0 j_0}}{\pi[r_{i_0 j_0 \to i_1 j_1}]^2} \to \nu'_{i_1 j_1} = \frac{\nu_{i_0 j_0}}{\pi[r_{i_0 j_0 \to i_1 j_1}]^2} \tag{13}$$

This energy could be concentrated in a space with radius ($l_{i_1 j_1}$):

$$E'_{i_1 j_{1,PURE}} = \frac{E_{i_0 j_0} \pi[\, l_{i_1 j_1}]^2}{\pi[r_{i_0 j_0 \to i_1 j_1}]^2} \to \nu'_{i_1 j_{1,PURE}} = \frac{\nu_{i_0 j_0} \pi[\, l_{i_1 j_1}]^2}{\pi[r_{i_0 j_0 \to i_1 j_1}]^2} \tag{14}$$

Some part of this energy could be absorbed by cells and molecules at these new points and cause their vibrations. We have:

$$E''_{i_1 j_1} = E'_{i_1 j_1} \otimes \pi[\, l_{i_1 j_1} - D_{i_1 j_1}]^2 = \frac{E_{i_0 j_0} \pi[\, l_{i_1 j_1} - D_{i_1 j_1}]^2}{\pi[r_{i_0 j_0 \to i_1 j_1}]^2}$$

$$\to \nu''_{i_1 j_1} = \nu'_{i_1 j_1} \pi[\, l_{i_1 j_1} - D_{i_1 j_1}]^2 = \frac{\nu_{i_0 j_0} \pi[\, l_{i_1 j_1} - D_{i_1 j_1}]^2}{\pi[r_{i_0 j_0 \to i_1 j_1}]^2} \tag{15}$$

In the above equation, ($l_{i_1 j_1}$) is the length of the effective space and ($D_{i_1 j_1}$) is the length of molecules at the point ($i_1 j_1$). Also, $E''_{i_1 j_1}$ is the energy absorbed by molecules at this point. Thus, to obtain the non-absorbed energy, we should subtract this energy from the initial one:

$$E_{i_1 j_{1,PURE}} = E'_{i_1 j_{1,PURE}} - E''_{i_1 j_1} \to \nu_{i_1 j_{1,PURE}} = \nu'_{i_1 j_{1,PURE}} - \nu''_{i_1 j_1}$$

$$\nu_{i_1 j_{1,PURE}} = \frac{\nu_{i_0 j_0} \pi[\, l_{i_1 j_1}]^2}{\pi[r_{i_0 j_0 \to i_1 j_1}]^2} - \frac{\nu_{i_0 j_0} \pi[\, l_{i_1 j_1} - D_{i_1 j_1}]^2}{\pi[r_{i_0 j_0 \to i_1 j_1}]^2} \tag{16}$$

This frequency corresponds to a source at point ($i_0 j_0$). However, the collision of these waves with charges on cells and molecules at point ($i_1 j_1$) lead to their vibrations. By the vibrations of these charges, some new waves emerge. These waves could be combined by the initial waves and produce new frequencies. We have:

$$\nu_{i_1 j_{1,TOT}} = \nu_{i_1 j_{1,PURE}} + \nu_{i_1 j_{1,EXCITED}} = \frac{\nu_{i_0 j_0} \pi[\, l_{i_1 j_1}]^2}{\pi[r_{i_0 j_0 \to i_1 j_1}]^2} - \frac{\nu_{i_0 j_0} \pi[\, l_{i_1 j_1} - D_{i_1 j_1}]^2}{\pi[r_{i_0 j_0 \to i_1 j_1}]^2} + \nu_{i_1 j_{1,EXCITED}} \tag{17}$$

This frequency is related to the first collision of the source waves with the molecules and neurons. Within the brain, there are many molecules, charges and cells which change the source waves and it is required that these calculations continue. For example, at the point ($i_N j_N$), we have:

$$\nu_{i_N j_{N,TOT}} = \frac{\nu_{i_{N-1} j_{N-1}} \pi[\, l_{i_N j_N}]^2}{\pi[r_{i_0 j_0 \to i_N j_N}]^2} - \frac{\nu_{i_{N-1} j_{N-1}} \pi[\, l_{i_N j_N} - D_{i_N j_N}]^2}{\pi[r_{i_0 j_0 \to i_N j_N}]^2} + \nu_{i_N j_{N,EXCITED}}$$

$$\frac{\left[\frac{\nu_{i_{N-2} j_{N-2}} \pi[\, l_{i_{N-1} j_{N-1}}]^2}{\pi[r_{i_0 j_0 \to i_{N-1} j_{N-1}}]^2} - \frac{\nu_{i_{N-2} j_{N-2}} \pi[\, l_{i_{N-1} j_{N-1}} - D_{i_{N-1} j_{N-1}}]^2}{\pi[r_{i_0 j_0 \to i_{N-1} j_{N-1}}]^2} + \nu_{i_{N-1} j_{N-1,EXCITED}}\right] \pi[\, l_{i_N j_N}]^2}{\pi[r_{i_0 j_0 \to i_N j_N}]^2}$$

$$-\frac{[\frac{\nu_{i_{N-2}j_{N-2}}\pi[\,l_{i_{N-1}j_{N-1}}]^2}{\pi[r_{i_0j_0\to i_{N-1}j_{N-1}}]^2}-\frac{\nu_{i_{N-2}j_{N-2}}\pi[\,l_{i_{N-1}j_{N-1}}-D_{i_{N-1}j_{N-1}}]^2}{\pi[r_{i_0j_0\to i_{N-1}j_{N-1}}]^2}+\nu_{i_{N-1}j_{N-1,EXCITED}}]\pi[\,l_{i_Nj_N}-D_{i_Nj_N}]^2}{\pi[r_{i_0j_0\to i_Nj_N}]^2}$$

$$+\nu_{i_Nj_{N,EXCITED}}$$

$$=\frac{\nu_{i_0j_0}\pi[\,l_{i_1j_1}]^2[\,l_{i_2j_2}]^2\ldots.[\,l_{i_{N-1}j_{N-1}}]^2[\,l_{i_Nj_N}]^2\,[1-\sum_{m=1}^{N}[\,l_{i_1j_1}-D_{i_1j_1}]^2\ldots\ldots\ldots[\,l_{i_mj_m}-D_{i_mj_m}]^2]}{\pi[r_{i_0j_0\to i_1j_1}]^2[r_{i_0j_0\to i_2j_2}]^2\ldots\ldots\ldots[r_{i_0j_0\to i_{N-1}j_{N-1}}]^2[r_{i_0j_0\to i_Nj_N}]^2}$$

$$-\frac{\nu_{i_0j_0}\pi[\,l_{i_1j_1}-D_{i_1j_1}]^2\ldots\ldots\ldots[\,l_{i_Nj_N}-D_{i_Nj_N}]^2[1+\sum_{m=1}^{N}\,l_{i_1j_1}]^2[\,l_{i_2j_2}]^2\ldots.[\,l_{i_{m-1}j_{m-1}}]^2[\,l_{i_mj_m}]^2\,]}{\pi[r_{i_0j_0\to i_1j_1}]^2[r_{i_0j_0\to i_2j_2}]^2\ldots\ldots..[r_{i_0j_0\to i_{N-1}j_{N-1}}]^2[r_{i_0j_0\to i_Nj_N}]^2}$$

$$+\nu_{i_1j_{1,EXCITED}}{}^{+}\ldots\ldots+\nu_{i_Nj_{N,EXCITED}}{}^{+}\ldots\ldots\ldots \quad (18)$$

The above equation shows that there is a significant difference between the source frequencies and observed ones. In fact, source waves could be taken many times by charges on cells and molecules and cause their excitations. Then, these excited molecules radiate new waves and this process continues between the neurons and electrodes. We can correct Eq (10) as below:

$$\bar{\nu}=\frac{\sum n_ix_j}{\sum_{i,j=1}^{N,X}n_ix_j}\otimes$$

$$[\frac{\nu_{i_0j_0}\pi[\,l_{i_1j_1}]^2[\,l_{i_2j_2}]^2\ldots.[\,l_{i_{N-1}j_{N-1}}]^2[\,l_{i_Nj_N}]^2\,[1-\sum_{m=1}^{N}[\,l_{i_1j_1}-D_{i_1j_1}]^2\ldots\ldots\ldots[\,l_{i_mj_m}-D_{i_mj_m}]^2]}{\pi[r_{i_0j_0\to i_1j_1}]^2[r_{i_0j_0\to i_2j_2}]^2\ldots\ldots..[r_{i_0j_0\to i_{N-1}j_{N-1}}]^2[r_{i_0j_0\to i_Nj_N}]^2}$$

$$-\frac{\nu_{i_0j_0}\pi[\,l_{i_1j_1}-D_{i_1j_1}]^2\ldots\ldots\ldots[\,l_{i_Nj_N}-D_{i_Nj_N}]^2[1+\sum_{m=1}^{N}\,l_{i_1j_1}]^2[\,l_{i_2j_2}]^2\ldots.[\,l_{i_{m-1}j_{m-1}}]^2[\,l_{i_mj_m}]^2\,]}{\pi[r_{i_0j_0\to i_1j_1}]^2[r_{i_0j_0\to i_2j_2}]^2\ldots\ldots..[r_{i_0j_0\to i_{N-1}j_{N-1}}]^2[r_{i_0j_0\to i_Nj_N}]^2}$$

$$+\nu_{i_1j_{1,EXCITED}}{}^{+}\ldots\ldots+\nu_{i_Nj_{N,EXCITED}}{}^{+}\ldots\ldots\ldots] \quad (19)$$

The above equation shows that the frequency received by the scopes is very different from the initial frequency, and contains information related to all interactions between neurons and molecules within the brain. Using Eq (9), we can obtain the dependency of the frequency on the charges and lengths:

$$\bar{\nu}=\frac{\sum n_ix_j}{\sum_{i,j=1}^{N,X}n_ix_j}[\frac{1}{(2\pi)^2}\sqrt{\frac{\lambda_{i_0j_0}\mu_0\pi l_{i_0j_0}}{m_{i_0j_0}}}\frac{Q_{i_0j_0}}{r_{i_0j_0}}\frac{l_{i_0j_0}}{T_{i_0j_0}}]\otimes$$

$$[\frac{\pi[\,l_{i_1j_1}]^2[\,l_{i_2j_2}]^2\ldots.[\,l_{i_{N-1}j_{N-1}}]^2[\,l_{i_Nj_N}]^2\,[1-\sum_{m=1}^{N}[\,l_{i_1j_1}-D_{i_1j_1}]^2\ldots\ldots\ldots[\,l_{i_mj_m}-D_{i_mj_m}]^2]}{\pi[r_{i_0j_0\to i_1j_1}]^2[r_{i_0j_0\to i_2j_2}]^2\ldots\ldots..[r_{i_0j_0\to i_{N-1}j_{N-1}}]^2[r_{i_0j_0\to i_Nj_N}]^2}$$

$$-\frac{\pi[\,l_{i_1j_1}-D_{i_1j_1}]^2\ldots\ldots\ldots[\,l_{i_Nj_N}-D_{i_Nj_N}]^2[1+\sum_{m=1}^{N}\,l_{i_1j_1}]^2[\,l_{i_2j_2}]^2\ldots.[\,l_{i_{m-1}j_{m-1}}]^2[\,l_{i_mj_m}]^2\,]}{\pi[r_{i_0j_0\to i_1j_1}]^2[r_{i_0j_0\to i_2j_2}]^2\ldots\ldots..[r_{i_0j_0\to i_{N-1}j_{N-1}}]^2[r_{i_0j_0\to i_Nj_N}]^2}$$

$$+\frac{1}{(2\pi)^2}\sqrt{\frac{\lambda_{i_1j_1}\mu_0\pi l_{i_1j_1}}{m_{i_1j_1}}}\frac{Q_{i_1j_1}}{r_{i_1j_1}}\frac{l_{i_1j_1}}{T_{i_1j_1}}+\ldots\ldots+\frac{1}{(2\pi)^2}\sqrt{\frac{\lambda_{i_Nj_N}\mu_0\pi l_{i_Nj_N}}{m_{i_Nj_N}}}\frac{Q_{i_Nj_N}}{r_{i_Nj_N}}\frac{l_{i_Nj_N}}{T_{i_Nj_N}}+\ldots\ldots\ldots] \quad (20)$$

The above frequency depends on all charges, the distance between the neurons, the length of the neurons or synapses, the interactions between the neurons and the excited frequencies. In addition to these parameters, we should add some extra parameters related to the interactions between the electrodes:

$$\bar{\nu}_{observed}=\bar{\nu}+\bar{\nu}_{noise,electrodes}=\frac{\sum n_ix_j}{\sum_{i,j=1}^{N,X}n_ix_j}[\frac{1}{(2\pi)^2}\sqrt{\frac{\lambda_{i_0j_0}\mu_0\pi l_{i_0j_0}}{m_{i_0j_0}}}\frac{Q_{i_0j_0}}{r_{i_0j_0}}\frac{l_{i_0j_0}}{T_{i_0j_0}}]\otimes$$

$$[\frac{\pi[\,l_{i_1j_1}]^2[\,l_{i_2j_2}]^2\ldots.[\,l_{i_{N-1}j_{N-1}}]^2[\,l_{i_Nj_N}]^2\,[1-\sum_{m=1}^{N}[\,l_{i_1j_1}-D_{i_1j_1}]^2\ldots\ldots\ldots[\,l_{i_mj_m}-D_{i_mj_m}]^2]}{\pi[r_{i_0j_0\to i_1j_1}]^2[r_{i_0j_0\to i_2j_2}]^2\ldots\ldots..[r_{i_0j_0\to i_{N-1}j_{N-1}}]^2[r_{i_0j_0\to i_Nj_N}]^2}$$

$$-\frac{\pi[\,l_{i_1j_1}-D_{i_1j_1}]^2\ldots\ldots\ldots[\,l_{i_Nj_N}-D_{i_Nj_N}]^2[1+\sum_{m=1}^{N}\,l_{i_1j_1}]^2[\,l_{i_2j_2}]^2\ldots.[\,l_{i_{m-1}j_{m-1}}]^2[\,l_{i_mj_m}]^2\,]}{\pi[r_{i_0j_0\to i_1j_1}]^2[r_{i_0j_0\to i_2j_2}]^2\ldots\ldots..[r_{i_0j_0\to i_{N-1}j_{N-1}}]^2[r_{i_0j_0\to i_Nj_N}]^2}$$

$$+\frac{1}{(2\pi)^2}\sqrt{\frac{\lambda_{i_1j_1}\mu_0\pi l_{i_1j_1}}{m_{i_1j_1}}}\frac{Q_{i_1j_1}}{r_{i_1j_1}}\frac{l_{i_1j_1}}{T_{i_1j_1}}+\ldots\ldots+\frac{1}{(2\pi)^2}\sqrt{\frac{\lambda_{i_Nj_N}\mu_0\pi l_{i_Nj_N}}{m_{i_Nj_N}}}\frac{Q_{i_Nj_N}}{r_{i_Nj_N}}\frac{l_{i_Nj_N}}{T_{i_Nj_N}}+\ldots\ldots\ldots]+\bar{\nu}_{noise,electrodes} \quad (21)$$

Now, the question that arises in the presence of these noises and extra interactions is how could we consider the activity of a part of the brain? To answer this question, we should indicate that we need to consider changes in the frequencies. This means that before a brain activity, we can measure the frequencies and after the brain activity, we can reconsider the frequencies. Then, by comparing them, we can obtain the desired results. For example, a minor change in a neuron charge may be multiplied by a factor, and produce a large change in the observed frequency. We have:

$$\delta Q_{i_0j_0}\to\overline{\delta\nu}_{observed}=\frac{\sum n_ix_j}{\sum_{i,j=1}^{N,X}n_ix_j}[\frac{1}{(2\pi)^2}\sqrt{\frac{\lambda_{i_0j_0}\mu_0\pi l_{i_0j_0}}{m_{i_0j_0}}}\frac{\delta Q_{i_0j_0}}{r_{i_0j_0}}\frac{l_{i_0j_0}}{T_{i_0j_0}}]\otimes$$

$$[\frac{\pi[\,l_{i_1j_1}]^2[\,l_{i_2j_2}]^2\ldots.[\,l_{i_{N-1}j_{N-1}}]^2[\,l_{i_Nj_N}]^2\,[1-\sum_{m=1}^{N}[\,l_{i_1j_1}-D_{i_1j_1}]^2\ldots\ldots\ldots[\,l_{i_mj_m}-D_{i_mj_m}]^2]}{\pi[r_{i_0j_0\to i_1j_1}]^2[r_{i_0j_0\to i_2j_2}]^2\ldots\ldots..[r_{i_0j_0\to i_{N-1}j_{N-1}}]^2[r_{i_0j_0\to i_Nj_N}]^2}$$

$$-\frac{\pi[\,l_{i_1j_1}-D_{i_1j_1}]^2\ldots\ldots\ldots[\,l_{i_Nj_N}-D_{i_Nj_N}]^2[1+\sum_{m=1}^{N}\,l_{i_1j_1}]^2[\,l_{i_2j_2}]^2\ldots.[\,l_{i_{m-1}j_{m-1}}]^2[\,l_{i_mj_m}]^2\,]}{\pi[r_{i_0j_0\to i_1j_1}]^2[r_{i_0j_0\to i_2j_2}]^2\ldots\ldots..[r_{i_0j_0\to i_{N-1}j_{N-1}}]^2[r_{i_0j_0\to i_Nj_N}]^2}$$

$$+\frac{1}{(2\pi)^2}\sqrt{\frac{\lambda_{i_1j_1}\mu_0\pi l_{i_1j_1}}{m_{i_1j_1}}}\frac{Q_{i_1j_1}}{r_{i_1j_1}}\frac{l_{i_1j_1}}{T_{i_1j_1}}+\ldots\ldots+\frac{1}{(2\pi)^2}\sqrt{\frac{\lambda_{i_Nj_N}\mu_0\pi l_{i_Nj_N}}{m_{i_Nj_N}}}\frac{Q_{i_Nj_N}}{r_{i_Nj_N}}\frac{l_{i_Nj_N}}{T_{i_Nj_N}}+\ldots\ldots\ldots]$$

$$\rightarrow \overline{\delta v}_{observed} = \delta Q_{i_0 j_0} \otimes \ \mathrm{H}\,(l_{i_m j_m}, D_{i_m j_m}, r_{i_0 j_0 \rightarrow i_m j_m}, \dots \dots) \tag{22}$$

where H is a function of all parameters including synaptic lengths, currents, separation distances and other neuronal properties. The above equation shows that only a very small change in a charge could cause a large change in observed frequencies. Thus, by comparing frequencies before an activity and after it, we can obtain the exact results about neurons.

Another question could be about the relation between the EEG frequencies and scalp thickness. Equation (20) shows that EEG frequencies depend on the distance between neuronal sources and electrodes, interacting molecules and cells between them, and the sizes of excited molecules. When a wave passing the scalp may be absorbed by molecules within it, it excites them and produces new waves. Also, some excited waves may join the initial source waves and produce new waves with new frequencies. Thus, the thickness of the scalp has a direct effect on EEG waves. we can write:

$$\delta l_{i_N j_N} \rightarrow \overline{\delta v}_{observed} = \frac{\sum n_i x_j}{\sum_{i,j=1}^{N,X} n_i x_j} [\frac{1}{(2\pi)^2} \sqrt{\frac{\lambda_{i_0 j_0} \mu_0 \pi l_{i_0 j_0}}{m_{i_0 j_0}}} \frac{Q_{i_0 j_0}}{r_{i_0 j_0}} \frac{l_{i_0 j_0}}{T_{i_0 j_0}}] \otimes$$

$$[\frac{\pi[\ l_{i_1 j_1}]^2 [\ l_{i_2 j_2}]^2 \dots . [\ l_{i_{N-1} j_{N-1}}]^2 [\ \delta l_{i_N j_N}]^2 \ [1 - \sum_{m=1}^{N} [\ l_{i_1 j_1} - D_{i_1 j_1}]^2 \dots \dots \dots [\ \delta l_{i_m j_m} - \delta D_{i_m j_m}]^2]}{\pi [r_{i_0 j_0 \rightarrow i_1 j_1}]^2 [r_{i_0 j_0 \rightarrow i_2 j_2}]^2 \dots \dots . [\delta r_{i_0 j_0 \rightarrow i_{N-1} j_{N-1}}]^2 [\delta r_{i_0 j_0 \rightarrow i_N j_N}]^2}$$

$$- \frac{\pi[\ l_{i_1 j_1} - D_{i_1 j_1}]^2 \dots \dots \dots [\ \delta l_{i_N j_N} - D_{i_N j_N}]^2 [1 + \sum_{m=1}^{N} \ l_{i_1 j_1}]^2 [\ l_{i_2 j_2}]^2 \dots . [\ \delta l_{i_{m-1} j_{m-1}}]^2 [\delta \ l_{i_m j_m}]^2 \ ]}{\pi [r_{i_0 j_0 \rightarrow i_1 j_1}]^2 [r_{i_0 j_0 \rightarrow i_2 j_2}]^2 \dots \dots . [\delta r_{i_0 j_0 \rightarrow i_{N-1} j_{N-1}}]^2 [\delta r_{i_0 j_0 \rightarrow i_N j_N}]^2}$$

$$+ \frac{1}{(2\pi)^2} \sqrt{\frac{\lambda_{i_1 j_1} \mu_0 \pi l_{i_1 j_1}}{m_{i_1 j_1}}} \frac{Q_{i_1 j_1}}{\delta r_{i_1 j_1}} \frac{\delta l_{i_1 j_1}}{T_{i_1 j_1}} + \dots \dots + \frac{1}{(2\pi)^2} \sqrt{\frac{\lambda_{i_N j_N} \mu_0 \pi \delta l_{i_N j_N}}{m_{i_N j_N}}} \frac{Q_{i_N j_N}}{\delta r_{i_N j_N}} \frac{\delta l_{i_N j_N}}{T_{i_N j_N}} + \dots \dots \dots]$$

$$\rightarrow \overline{\delta v}_{observed} = \prod [\delta \ l_{i_n j_n}]^2 \prod [\delta r_{i_0 j_0 \rightarrow i_{n-1} j_{n-1}}]^{-2} \otimes \ \mathrm{Y}\,(l_{i_m j_m}, D_{i_m j_m}, r_{i_0 j_0 \rightarrow i_m j_m}, \dots \dots) \tag{23}$$

where Y is a function of brain parameters. The above equation shows that any change in the thickness of the scalp may cause a large change in EEG frequencies. Thus, observed frequencies for different ages are different.

To test this generalized version, we can reconsider the results of [14]. In this research, based on the response to sleep deprivation, low-delta (0.5–1 Hz) and mid-delta activity (1.25–2 Hz) were discussed. It was shown that sleep deprivation resulted in an increase in source strength only for mid-delta activity, mainly in the parietal and frontal regions. Low-delta activity dominated in occipital and temporal regions, and mid-delta activity in limbic and frontal regions independent of the level of sleep pressure. These results are consistent with our model. Because the sizes of parietal and frontal regions are different from the sizes of the occipital and temporal regions, their emitted frequencies are different. Also, the number of neuronal cells, charges and molecules within the parietal and frontal regions are different from the number of neuronal cells, charges and molecules of the occipital and temporal regions. For example, the volume of the frontal lobe is approximately more than temporal lobe and consequently, more waves could be emitted by its neurons (See table 1). Although, in addition to the size and volume, other parameters like the number of cells, molecules and charges are also important. For example, maybe one region has lower volume but it may radiate higher frequencies of waves. As

a result, it is natural that these regions emit different ranges of frequencies.

Table 2. Dependency of frequencies on the volume of the brain sections.

Total Frontal Lobe	Total Temporal Lobe
260503 mm^3	251609 mm^3
mid-delta (1.25–2 Hz)	low-delta (0.5–1 Hz)

5. Conclusion

In this paper, we have proposed a model which relates the EEG topographic parameters to the number of interacting neurons, lengths of synapses+sizes of neurons, charges and masses of ions and particles, and radii of circles in which interactions occur. In this model, charges move along neurons or between axons and dendrites, and emit some waves. These waves are absorbed by electrodes and produce topographic images. By analyzing the densities of the waves on these pictures, we can estimate the charge, mass and type of exchanged particles and number of interacting neurons. We have tested the model against data.

In addition, we have generalized the model to consider the effects of other neurons, molecules and charges. We have shown that the energy of any propagated wave is divided on a circle and some part of it is absorbed by neurons and molecules. These molecules and cells may be excited and emit new waves with new frequencies. These new frequencies may add to the initial frequencies and produce new waves. These waves also propagate and their energies are divided on new bigger circles. Again, some cells absorb these waves, are excited and emit new waves. This process continues from the source point to the electrodes. Thus, the observed frequency may be different from the initial frequency. However, any change in one parameter within the brain could cause a large change in observed frequency. Thus, by considering the frequencies before and after a brain activity, we can analyze the evolution of the neurons. We also showed that the thickness of the scalp in different ages and different parts of the brain has a direct effect on EEG frequencies.

Data availability

Not applicable. This is a theoretical model which has been tested by the data of previous experiments in the cited references.

Conflict of interest

The authors declare there is no conflict of interest.

References

1. A. Mucci, A. Üçok, M. Ø. Nielsen, Electrophysiological and neuroimaging research on negative symptoms: Future challenges, *Clin. EEG Neurosci.,* **49** (2018), 3–5. https://doi.org/10.1177/1550059417748074
2. F. C. Morabito, D. Labate, F. L. Foresta, A. Bramanti, G. Morabito, I. Palamara, Multivariate multi-scale permutation entropy for complexity analysis of Alzheimer's disease EEG, *Entropy,* **14** (2012), 1186–1202. https://doi.org/10.3390/e14071186

3. D. F. Salisbury, Stimulus processing awake and asleep: Similarities and differences in electrical CNS responses, in *Sleep onset: Normal and abnormal processes* (eds. R. D. Ogilvie and J. R. Harsh, American Psychological Association, (1994), 289–308. https://doi.org /10.1037/10166-017
4. F. C. Morabito, D. Labate, A. Bramanti, F. La Foresta, G. Morabito, I. Palamara, et al., Enhanced compressibility of EEG signal in Alzheimer's disease patients, *IEEE Sensors J.*, **13** (2013), 3255–3262. https://doi: 10.1109/JSEN.2013.2263794
5. F. C. Morabito, D. Labate, G. Morabito, I. Palamara, H. Szu, Monitoring and diagnosis of Alzheimer's disease using noninvasive compressive sensing EEG, in *Proc. SPIE 8750, Independent Component Analyses, Compressive Sampling, Wavelets, Neural Net, Biosystems, and Nanoengineering XI, 87500Y*, (2013). https://doi.org/10.1117/12.2020886
6. A. Mucci, U. Volpe, E. Merlotti, P. Bucci, S. Galderisi, Pharmaco-EEG in Psychiatry, *Clin. EEG Neurosci*., **37** (2006), 81–98. https://doi:10.1177/155005940603700206
7. M. Christoph, T. K Michel, EEG microstates as a tool for studying the temporal dynamics of whole-brain neuronal networks: A review, *NeuroImage*, **180** (2018), 577–593. https://doi.org/10.1016/j.neuroimage.2017.11.062.
8. A. Jabès, G. Klencklen, P. Ruggeri, C. M. Michel, P. B. Lavenex, P. Lavenex, Resting-state EEG microstates parallel age-related differences in allocentric spatial working memory performance, *Brain Topogr.,* **34** (2021), 442–460. https://doi.org/10.1007/s10548-021-00835-3
9. L. Bréchet, D. Brunet, L. Perogamvros, G. Tonini, C. M. Michel, EEG microstates of dreams, *Sci. Rep.,* **10** (2020), 17069. https://doi.org/10.1038/s41598-020-74075-z
10. W. J. Bosl, H. Tager-Flusberg, C. A. Nelson, EEG analytics for early detection of autism spectrum disorder: A data-driven approach, *Sci. Rep.,* **8** (2018), 6828. https://doi.org/10.1038/s41598-018-24318-x
11. T. H. Pham, J. Vicnesh, J. K. E. Wei, S. L. Oh, N. Arunkumar, E. W. Abdulhay, et al., Autism spectrum disorder diagnostic system using HOS Bispectrum with EEG signals., *Int. J. Environ. Res. Public Health,* **17** (2020), 971. https://doi.org/10.3390/ijerph17030971
12. V. Bairagi, EEG signal analysis for early diagnosis of Alzheimer disease using spectral and wavelet based features, *Int. J. Inf. Tecnol.,* **10** (2018), 403–412. https://doi.org/10.1007/s41870-018-0165-5
13. A. Markovic, P. Achermann, T. Rusterholz, L. Tarokh, Heritability of sleep EEG topography in adolescence: Results from a longitudinal twin Study, *Sci. Rep.,* **8** (2018), 7334. https://doi.org/10.1038/s41598-018-25590-7
14. A. Bersagliere, R. D. Pascual-Marqui, L. Tarokh, P. Achermann, Mapping slow waves by EEG topography and source localization: Effects of sleep deprivation, *Brain Topogr.,* **31** (2018), 257–269. https://doi.org/10.1007/s10548-017-0595-6
15. B. Kim, E. Hwang, R. E. Strecker, J. H. Choi, Y. Kim, Differential modulation of NREM sleep regulation and EEG topography by chronic sleep restriction in mice, *Sci. Rep*., **10** (2020). https://doi.org/10.1038/s41598-019-54790-y
16. M. A. Rahman, A. Anjum, M. M. H. Milu, F. Khanam, M. S. Uddin, M. N. Mollah, Emotion recognition from EEG-based relative power spectral topography using convolutional neural network, *Array*, **11** (2021), 100072. https://doi.org/10.1016/j.array.2021.100072
17. M. Xu, J. Yao, Z. Zhang, R. Li, B. Yang, C. Y. Li, et al., Learning EEG topographical representation for classification via convolutional neural network, *Pattern Recogn.*, **105** (2020), 107390. https://doi.org/10.1016/j.patcog.2020.107390

18. S. Scarpelli, C. Marzano, A. D'Atri, M. Gorgoni, M. Ferrara, L. De Gennaro, State- or trait-like individual differences in dream recall: Preliminary findings from a within-subjects study of multiple nap REM sleep awakenings, *Front. Psychol.,* **6** (2015), 928. https://doi.org/10.3389/fpsyg.2015.00928

AIMS Press